Jungsuk Kim*
Joachim Ulrich

Thermodynamic Study on the Amorphous Form and Crystalline Hydrates Using in Situ Raman and FBRM

The solubilities and maximum supersaturation concentrations of an amorphous and the crystalline tetrahydrate and heptahydrate solids of disodium guanosine 5'-monophosphate (GMP) in water-methanol mixtures were measured in situ by Raman spectroscopy and focused beam reflectance measurement. The distinct Raman peaks of the amorphous form, crystalline hydrates, solution, and solvent were used for measurements of solubility and maximum supersaturation. Above 45 °C and at methanol fractions of 0.15–0.90, the tetrahydrate was the stable form, while below 40 °C and at methanol fractions of 0.15–0.60, the heptahydrate was the stable form. Especially, the tetrahydrate was stable in the methanol fraction > 0.7 at the temperature investigated. The solubility and supersaturated concentration values can be used to selectively produce amorphous, tetrahydrate, and heptahydrate solids of GMP by anti-solvent crystallization.

Supporting Information available online

Keywords: Amorphous solids, Disodium guanosine 5'-monophosphate, Hydrates, Solubility, Supersaturation

Received: June 18, 2021; *revised:* November 08, 2021; *accepted:* December 06, 2021

DOI: 10.1002/ceat.202100260

1 Introduction

During a crystallization process, operation, and storage of polymorphs including solvates (hydrates), polymorphic transformation may occur [1, 2]. To analyze the phenomenon of hydrate state change, information is required on the solubility and supersaturation limits (upper limit of the metastable zone) of each crystalline form [3].

Disodium guanosine 5'-monophosphate (GMP) is an important material used for preparing ribonucleic acids (RNA), and it is also used as intermediate in drug synthesis and as food additive. It is synthesized by fermentation and then crystallized from the fermentation broth, which contains many impurities. The crystallization serves to control product qualities such as the hydrate forms and the purity. GMP is known to have one amorphous form and several crystalline forms, which include the tetrahydrate form and the heptahydrate form [4, 5]. The chemical structures of the GMP tetrahydrate and heptahydrate are shown in the Supporting Information (Fig. S1). To understand its polymorph transformation, the solubility of the polymorphs and supersaturation of the solution should be determined. Furthermore, previous studies on GMP crystallization focused mainly on the transformation of the heptahydrate and amorphous forms [6, 7]. Several papers reported the solubility of GMP with different anti-solvents, temperatures, and pH values [8–10]. However, these studies were limited to the amorphous and heptahydrate forms; therefore, studies on the solubility of the polymorphic forms of GMP and crystallization of the tetrahydrate crystals are lacking. Thus, the objective of this study is to determine the solubility and supersaturation limit for crystallization of the tetrahydrate.

Supersaturation is a non-equilibrium parameter that affects the nucleation and crystal growth kinetics of the polymorphic forms [11–13]. Supersaturation is calculated by the solubility and real solution concentration. Therefore, the solubility of the polymorphic forms is very important and must be measured to understand a crystallization process [14]. This study reveals the thermodynamic properties and formation conditions for the amorphous, heptahydrate, and tetrahydrate forms of GMP.

The residual solid in the solubility measurement and analysis might be transformed. Therefore, in situ measurement techniques are desirable because it is difficult to monitor the metastable form with an off-line analysis [15–17]. In this study, a focused beam reflectance measurement (FBRM) probe and a Raman spectroscope were mounted on-line to measure the crystal size, the number of particles, the polymorph difference, and the solubility, simultaneously. In addition, off-line measurements using thermogravimetric analysis-differential scanning calorimetry (TGA-DSC), powder X-ray diffraction (PXRD), light microscopy, Raman spectroscopy, and scanning electron microscopy (SEM) revealed the thermal decomposition properties, structure, and crystal form of GMP. This study

Jungsuk Kim, Prof. Joachim Ulrich
click7031@naver.com
ehem. Zentrum für Ingenieurwissenschaften, Martin-Luther-Universität Halle-Wittenberg, 06099 Halle, Germany.

revealed the crystallization and solubility of the tetrahydrate crystals. It is expected that the solubility information of the amorphous solid, the tetrahydrate, and the hexahydrate will greatly contribute to the control of the purity of crystals and the selective production of GMP hydrates. The solubility of the crystalline and amorphous forms in solvent mixtures of various compositions in the range of 293.15–333.15 K was studied.

Solubility must be measured simultaneously with the analysis of the crystalline form because transformation from the metastable form to the stable form may occur in the solid phase. Analysis of the crystalline form should be accompanied by the solubility measurement because changes in the crystalline form may depend on the temperature and the solvent fraction. In previous studies, the solubility had been measured by the gravimetric method, but changes in the crystal form during the measurement process were not analyzed [8–10]. Therefore, the solubility of GMP was measured in situ by Raman spectroscopy using calibration plots, and the effects of the temperature and the solvent fraction on the solubility were measured for the solid forms.

When the amorphous form is suspended in a saturated solution, a transformation to the stable form can occur. Thus, there can be difficulties in measuring the solubility of the unstable form. To know the maximum supersaturation limit in anti-solvent crystallization is also necessary for selective crystallization of GMP polymorphs. From thermal and PXRD analyses, GMP is known to crystallize both as the tetrahydrate and the heptahydrate form [18]. However, because of the difficulty of crystallization caused by gel formation through tetramer stacking, only the crystal structure of the heptahydrate has been reported [5, 19]. The crystal structure of the tetrahydrate was disclosed with intermediate phases [20]. An understanding of the selective crystallization of GMP hydrates requires solubility and supersaturation limits, and these have rarely been reported for the tetrahydrate, heptahydrate, and the amorphous solid [6–8].

In this work, an in-situ measurement of the solubility, supersaturated concentration, solid form, crystal size, and number of particles was carried out by FBRM and Raman spectroscopy. The solubilities of the amorphous, tetrahydrate, and heptahydrate forms in mixed solvents of methanol/water were measured at a certain temperature and a certain solvent fraction. The thermodynamic properties and formation conditions for the amorphous, heptahydrate, and tetrahydrate forms were revealed. The solubility and supersaturation limit for tetrahydrate crystallization was studied. The dependence of the relative stability of the amorphous, tetrahydrate, and heptahydrate forms on the solvent composition and the temperature as well as thermodynamic properties, such as the enthalpy and entropy of dissolution of GMP, were estimated by plotting the solubility data and temperature using the van't Hoff equation. Finally, the supersaturated concentrations and solubilities of polymorphic GMP for various temperatures and solvent fractions were successfully determined by in-situ Raman spectroscopy and FBRM.

2 Experimental Section

2.1 Materials

GMP was supplied by Wako Pure Chemical Industries with a mole fraction purity of 99.9 wt %. In this study, the heptahydrate GMP used was prepared by recrystallization by adding methanol to the GMP solution dissolved in water at 20 °C. Methanol was of analytical grade and purchased from Aldrich, USA. Distilled water was used.

2.2 Preparation of Amorphous GMP

An amorphous form was produced by anti-solvent crystallization using water and methanol. After 25 g of the hydrate crystals was dissolved in 100 g water at 20 °C, the solution was supersaturated by adding 50 g methanol for 10 s. During the experiments, the Raman peaks were recorded at intervals of 5 s to monitor the amorphous form. Before transformation, the solids were separated by using a solid-liquid separator with a glass filter, washed with methanol, and dried at 30 °C for 2 h. PXRD and Raman spectroscopy were used to confirm the polymorphic forms and hydrate forms of the product. The purity of the prepared amorphous form was above 0.95 in the mass fraction from the Raman peak.

2.3 Tetrahydrate and Heptahydrate Preparation

Tetrahydrate crystals were obtained in 70 % methanol/30 % water at 50 °C. Heptahydrate crystals were prepared by anti-solvent crystallization with 50 % methanol/50 % water at 30 °C. Raman spectroscopy was used to monitor the hydrate forms in situ at intervals of 5 s. The crystals were separated by using a solid-liquid separator with a glass filter and dried at 30 °C for 2 h. It was confirmed that the hydrate crystals were not transformed during drying. XRD and Raman spectroscopy were used to confirm the polymorphic form of the product. The purity of the prepared hydrate was above 0.99 in the mass fraction from the Raman peak.

2.4 Solubility Measurement Method

The gravimetric method was used to measure the solubility. During the measurement of the polymorph solubility, the crystalline form of the residual solid can undergo transformation. A phase transition of the metastable form in the solution phase may occur during the solubility measurement process [15, 21]. The solubility of the metastable form cannot be measured by an off-line method. Therefore, an on-line measurement is desirable since it is impossible to monitor the transformation of the crystalline form during off-line analysis.

The measuring device consists of an FBRM probe (Mettler-Toledo, Switzerland) and a Raman spectrometer (Kaiser Optical Systems, Ann Arbor MI, USA), which are in-situ measuring instruments. In-situ Raman measurements of the solid polymorph concentration and the solution concentration were used

to measure simultaneously the solubility, the solid concentration, and a potential change in the polymorph of GMP with elapsed time. The equilibrium point was finally obtained; at the same time, the polymorph of the residual solid was measured in situ. The GMP solids, solution, and solvent had characteristic Raman spectra, from which the Raman spectra of the solution that did not overlap with others were selected to develop the calibration curve for the solution concentration.

The setup of the solubility measurement apparatus is shown in Fig. 1. It consists of a Raman spectrometer and an FBRM probe, used in conjunction with a temperature controller (±0.1 °C) in a jacketed vessel. The double-jacket glass was connected with a thermostat (RAUDA, K-4/R) with an accuracy of 0.1 K and kept at a constant temperature. The vessel was equipped with a magnetic driver and condenser to prevent any vapor leakage. In-situ measurements of the solid and solution concentrations were used to obtain the solubility measurements. In the in-situ Raman method, it is necessary to search for the point of equilibrium under isothermal conditions, where the concentration is varied for different conditions. Linear relationships with the concentration of the solution and the Raman intensity were used to measure the solubility of the GMP in binary solvent mixtures (Fig. S5).

Solute was added step by step until saturation was reached. Then, an additional 5–10 g of extra solute was added per 100 g of saturated solution. The solubility of the solute at a given temperature was calculated from the weight of the dissolved solute in the solvent. The temperature was set in the range from 20 to 60 °C. Off-line analysis of the final sample was carried out with an in-situ measurement. After 48 h, the remaining solid was filtered and weighed, and the concentration calculated as gram of dissolved solute per gram of solvent. The off-line data were confirmed by the Raman data. Unstable forms such as the amorphous form changed easily into a stable form during the solubility measurement. Some of the experiments were conducted in triplicate to check the reproducibility. The solubility for a given temperature was reproducible within 0.001 g of solute per 100 g of solution. The off-line measurement was performed twice and compared with the in-line measurement result. Thus, the accuracy for the solubility measurement was in the range of 99.9–99.99 %.

2.5 Raman Spectroscopy and Powder X-Ray Diffraction

The Raman spectra were recorded using RXN Systems (Kaiser Optical Systems, USA) equipped with a light-emitting diode laser (785 nm, 450 mW) as the excitation source. A one-fold objective lens with a probe was used to collect the spectra. The spectra ranged from 100 to 1890 cm^{-1} and were acquired with 4 cm^{-1} of spectral width and 5 s of exposure. The iCRaman software (Mettler-Toledo, Switzerland) was used to calibrate the concentrations of solids and solution. Analysis of the Raman data was performed by the absence and occurrence of peaks originally found in spectra of the single components (see Fig. S3). To calibrate the concentrations of the solids and solution, a multivariate partial least square (PLS) model was used.

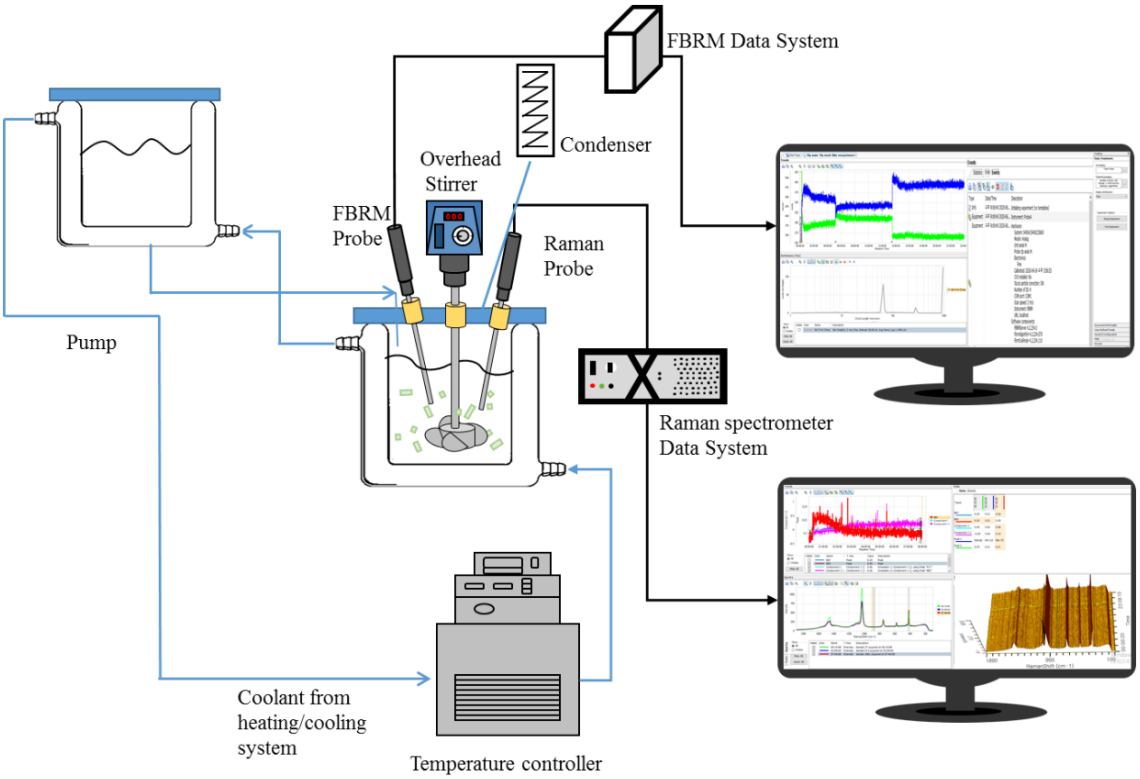

Figure 1. Setup of the experimental apparatus.

For PXRD, a PXRD pattern of the solid was calculated using a Smart Lab X-ray diffractometer (Rigaku, Japan) with CuKα radiation generated at 200 mA and 45 kV. The sample was placed on a silicone plate at room temperature. Data were collected from 3° to 45° (2θ) at a step size of 0.02° and a scan rate of 5° min^{-1}.

2.6 Focused Beam Reflectance Measurement

An FBRM probe (model M400LF; Mettler-Toledo, USA) was used to characterize both the nucleation and dissolution of the material. FBRM measures a chord length distribution (CLD) and thereby the number and the measured count data can be split into specific population regions in the size range, as the cord length is converted into particle sizes. As the FBRM was carried out over a 10-s period, the number of counts in the range of 0.1–990 µm was used as an indication of nucleation. The process of crystalline transformation was also monitored by monitoring the changes in the size and number of particles. The solubilities of the amorphous and hydrate forms, which can change into a more stable form, were determined by FBRM.

2.7 Thermal Analysis

TGA and DSC of the solid forms were carried out by using a thermogravimetric analyzer (TGA 2050, DSC 2010; TA Instruments, USA) at up to 573 K with dried nitrogen and at a flow rate of 70 mL min^{-1} and a heating rate of 10 K min^{-1}.

The characterization of the materials and the calibration of the Raman spectroscopic data are given in detail in the Supporting Information.

3 Results and Discussion

3.1 Solubilities of the Amorphous, Tetrahydrate, and Heptahydrate Solids

Solubility (equilibrium state) is a very important thermodynamic parameter for determining the crystallization mode, supersaturation, phase diagram, and yields [22, 23]. The solubility is the concentration at which no crystalline state change can be observed. In addition, it can also affect the kinetics of crystallization and the particle size and shape, which are controlled by the supersaturation. The solubility measured by the off-line gravimetric method was compared with the solubility measured by Raman spectroscopy. Raman spectroscopy in-situ monitored the measurement by the gravimetric method. In the final data of the experimental runs, the results of the Raman spectroscopy were well matched with those of the solubility measured off-line. This method was then repeated to measure the amorphous, heptahydrate, and tetrahydrate equilibrium solubilities at different temperatures. Solubility and transformation were easily detected from the Raman peak and FBRM data. The solid concentration, solution concentration, and solubility were measured in the binary solvent mixture in situ by Raman spectroscopy. Examples of the solubility measurement at a certain methanol mass fraction and temperature are shown in Fig. 2.

The solubilities of the amorphous and heptahydrate particles/crystals measured by Raman spectroscopy are shown in Fig. 3a with its waterfall diagram. To measure the solubility of the heptahydrate solid, an excess amount was added. After measurement, Raman spectroscopy at 20 °C and a methanol mass fraction of 0.5 were used to confirm the form of the residue. A change in crystal form during measurement was observed. Of amorphous solid, 15 g was added to 100 g of solvent. After the addition, the amorphous solid started to dissolve. At equilibrium, 4.954 g of solid was dissolved and 10.045 g of solid did not dissolve. After about 20 h, the amount of the amorphous solid started to decrease sharply as it was transformed into heptahydrate crystals. With an increase in the amount of heptahydrate crystals in the transformation process, the solution concentration decreased to 0.0263 g g^{-1}. As a result, the solubility of the amorphous form was 0.04951 g g^{-1}, and the solubility of the heptahydrate was 0.0263 g g^{-1}. This is because the heptahydrate is more thermodynamically stable than the amorphous solid in these solvents. The solubilities of the heptahydrate and tetrahydrate crystals measured by Raman spectroscopy at 50 °C and a methanol mass fraction of 0.7 are shown in Figs. 3b and 3c. Of the heptahydrate solid, 20 g was added to 100 g of solvent. At equilibrium, 4.205 g of heptahydrate had dissolved in 100 g of solvent. At about 6844 s, the heptahydrate crystal started to be transformed into the tetrahydrate crystal. The Raman waterfall at the same condition shows that the Raman shift of 893 cm^{-1} (heptahydrate) disappeared at 8238 s and the one of 882 cm^{-1} (tetrahydrate) appeared at 6844 s. This indicates that the heptahydrate in

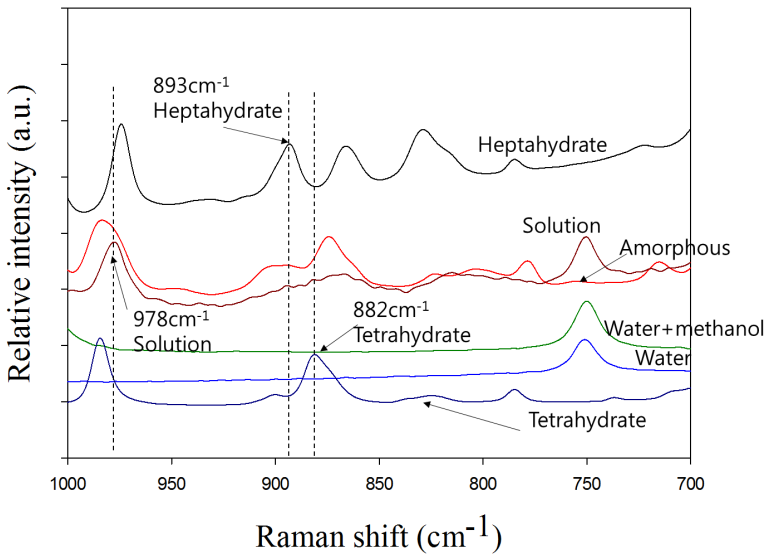

Figure 2. Characteristic Raman spectra of the amorphous solid, tetrahydrate crystal, heptahydrate crystal, solution and solvent ranging from 700 to 1000 cm^{-1}.

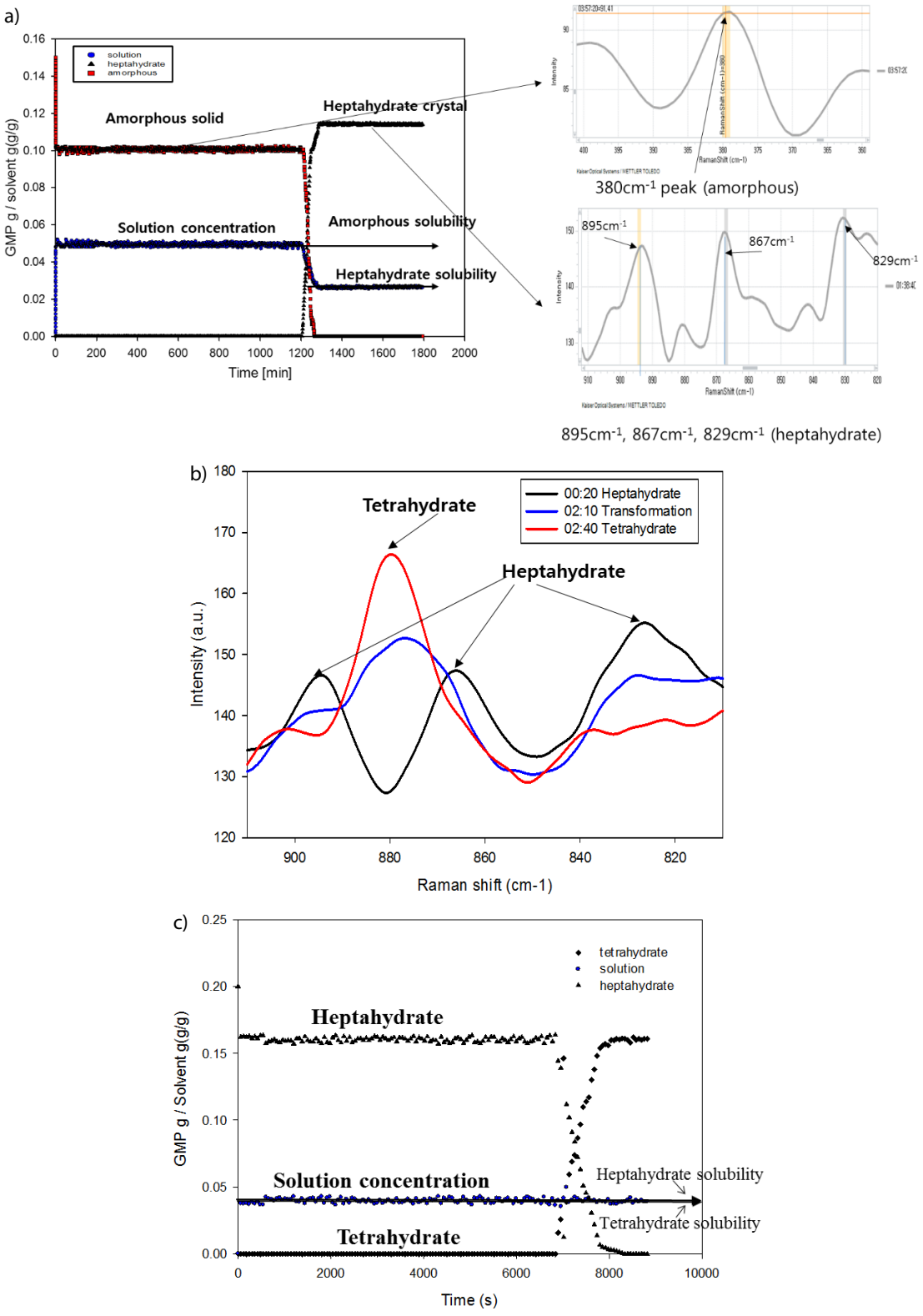

Figure 3. (a) Solubility measurement of the amorphous solid (metastable form) and heptahydrate (stable form) in binary solvent mixtures measured by Raman spectroscopy at 293.15 K and a methanol fraction of 0.5 with Raman spectra. (b, c) Solubility measurement of the heptahydrate (metastable form) and the tetrahydrate (stable form) in binary solvent mixtures measured by Raman spectroscopy at 323.15 K and a methanol fraction of 0.7 with Raman spectra of the solid forms.

binary solvent mixtures (methanol + water) was transformed to the tetrahydrate for 1394 s. As the tetrahydrate crystals increase in the transformation process, the solution concentration decreases to 0.04205 g. As a result, the solubilities of the heptahydrate and tetrahydrate are almost the same. However, the tetrahydrate is a little more thermodynamically stable than the heptahydrate in methanol/water.

The solubility of the stable form for the amorphous, tetrahydrate, and heptahydrate solids in water/methanol was determined in the range of 20–60 °C and a methanol mass fraction of 0.1–0.9. Experiments for the stable-form solubility were carried out for about 48 h. The experimental data are listed in Tab. 1 and plotted in Fig. 4, in which the solubility of GMP is expressed as the mass of GMP per mass of solvent. According to a previous work [8], the solubility of the heptahydrate in a methanol fraction of 0.3 was found to be 0.0395 g g^{-1} at 20 °C. This is similar to the data measured in this study. The solubility increased slightly with increasing temperature, as shown in Fig. 4, because the solubility strongly depends on the solvent fraction in water/methanol. Anti-solvent crystallization using methanol can be applied to a selective preparation of GMP. Furthermore, the solubility curve is divided into two zones: at 50–60 °C and 0.15 < methanol fraction < 0.9, the tetrahydrate is stable, while below 40 °C and at 0.15 < methanol fraction < 0.6, the heptahydrate is stable. At 20–60 °C and a methanol fraction of 0.8–0.9, the tetrahydrate is stable. At methanol fractions < 0.1 and all temperatures, the amorphous form was found, even though heptahydrate solids were added in the experiment. Crystals of the tetrahydrate were obtained at temperatures > 45 °C. At high temperatures, crystals with low hydration numbers are easily formed, and ionic groups are not fully hydrated under these conditions. The solubility of the amorphous solid is highest at the temperatures investigated. The amorphous solids were formed at the temperatures investigated and a water fraction of > 0.9, and the solubility of the amorphous solids was highest within this temperature range.

As a result, the solubility (equilibrium) and the concentration at which solids start to form (metastable zone limit) are found by simultaneously measuring the solution concentration and the concentrations of the tetrahydrate, heptahydrate, and amorphous solids.

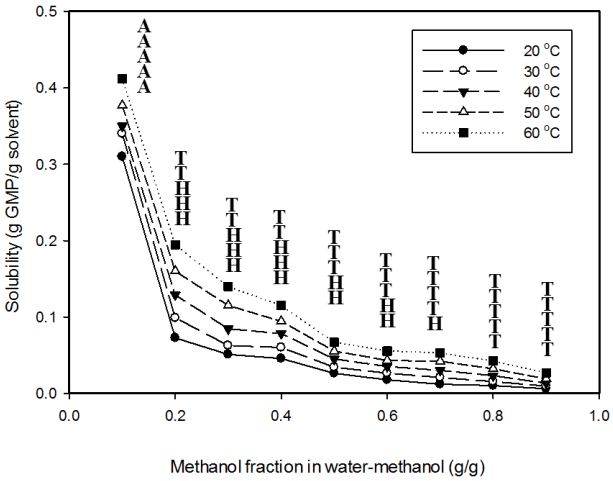

Figure 4. Solubility of GMP in water/methanol at various temperatures and methanol fractions.

This equilibrium water activity value depends greatly on the temperature. The lower the temperature, the smaller is the water activity value needed to attain equilibrium between the hydrates. The obtained results are useful for determining the crystallization parameters to achieve the desired hydrates. The approach can be applied to other amorphous and hydrate systems.

Intermediate phases were detected during transformation from the amorphous to the hydrate form. Amorphous solids are dissolved because of the solubility difference, and the hydrates are crystallized. In addition, the water molecules of the heptahydrate are desorbed below about 40 °C, and the heptahydrate is transformed into the tetrahydrate because of hydration loss. This supports our understanding that a single

Table 1. Solubility of the stable form as a function of the temperature and solvent fraction. A, amorphous; H, heptahydrate; T, tetrahydrate. Errors of measurements were less than 0.1 %.

T [°C]	Methanol mass fraction [–]								
	0.1	0.2	0.3	0.4	0.5	0.6	0.7	0.8	0.9
20	0.3102 (A)	0.07255 (H)	0.05103 (H)	0.04563 (H)	0.02634 (H)	0.01792 (H)	0.01213 (H)	0.01022 (T)	0.00612 (T)
25	0.3287 (A)	0.08315 (H)	0.06051 (H)	0.05055 (H)	0.03010 (H)	0.02153 (H)	0.01642 (H)	0.01312 (T)	0.00745 (T)
30	0.3418 (A)	0.09891 (H)	0.06263 (H)	0.06018 (H)	0.03421 (H)	0.02647 (H)	0.02086 (T)	0.01546 (T)	0.00953 (T)
35	0.3435 (A)	0.1172 (H)	0.07758 (H)	0.07070 (H)	0.03844 (H)	0.03046 (T)	0.02355 (T)	0.01878 (T)	0.01123 (T)
40	0.3488 (A)	0.1291 H)	0.08445 (H)	0.07840 (H)	0.04491 (T)	0.03523 (T)	0.03027 (T)	0.02316 (T)	0.01333 (T)
45	0.3606 (A)	0.1432 (T)	0.09965 (T)	0.08935 (T)	0.04965 (T)	0.03985 (T)	0.03582 (T)	0.02812 (T)	0.01658 (T)
50	0.3771 (A)	0.1602 (T)	0.11510 (T)	0.09431 (T)	0.05548 (T)	0.04312 (T)	0.04240 (T)	0.03218 (T)	0.01887 (T)
55	0.3968 (A)	0.1789 (T)	0.12840 (T)	0.1044 (T)	0.06032 (T)	0.04915 (T)	0.04673 (T)	0.03665 (T)	0.02375 (T)
60	0.4125 (A)	0.1945 (T)	0.14010 (T)	0.1157 (T)	0.06680 (T)	0.05543 (T)	0.05325 (T)	0.04223 (T)	0.02682 (T)

intermediate state composed of tetrahydrate was observed with the dehydration test [18].

From the solubility data, the enthalpy of dissolution, ΔH_d[1)], and the entropy of dissolution, ΔS_d, can be calculated [24].

$$\ln x = -\frac{\Delta H_d}{RT} + \frac{\Delta S_d}{R} \quad (1)$$

where R is the gas constant, ΔH_d and ΔS_d are the dissolution enthalpy and the entropy, respectively, and T is the absolute temperature.

Examples of the solubilities of the tetrahydrate and heptahydrate, which are plotted as ln$x$ versus 1/T for solvent fractions, are shown in Fig. 5. The values of the enthalpy and entropy of dissolution of both forms were obtained from the slope and the intercept of the plots and are listed in Tab. 2. The values of the enthalpy and entropy of dissolution of the heptahydrate were higher than those of the tetrahydrate. A similar result was reported for the anhydrate/monohydrate of carbamazepine in water-methanol mixtures [25]. However, the enthalpy and entropy of dissolution of both the tetrahydrate and heptahydrate increased with increasing water fraction in the solvent mixture. The enthalpy and entropy of dissolution also increased with increasing methanol fraction in the solvent, as the solubility in water was much higher than that in methanol. The relative stabilities of the tetrahydrate and heptahydrate can be obtained from Fig. 5, and enantiotropic behavior is exhibited. For a solvent fraction, the stable form must have a lower solubility than the metastable form.

The intercept in the extrapolation of the plots of the two forms represents the point where the solubilities of the tetrahydrate and heptahydrate are identical. In other words, the tetrahydrate and heptahydrate are in equilibrium; thus, it is referred to as the transition temperature in the specified solvent system. The tetrahydrate is the stable form at temperatures higher than the transition point; the heptahydrate is the stable form if the temperature is lower than the transition point. A smaller water fraction leads to a lower transition temperature between heptahydrate and tetrahydrate, but the tetrahydrate

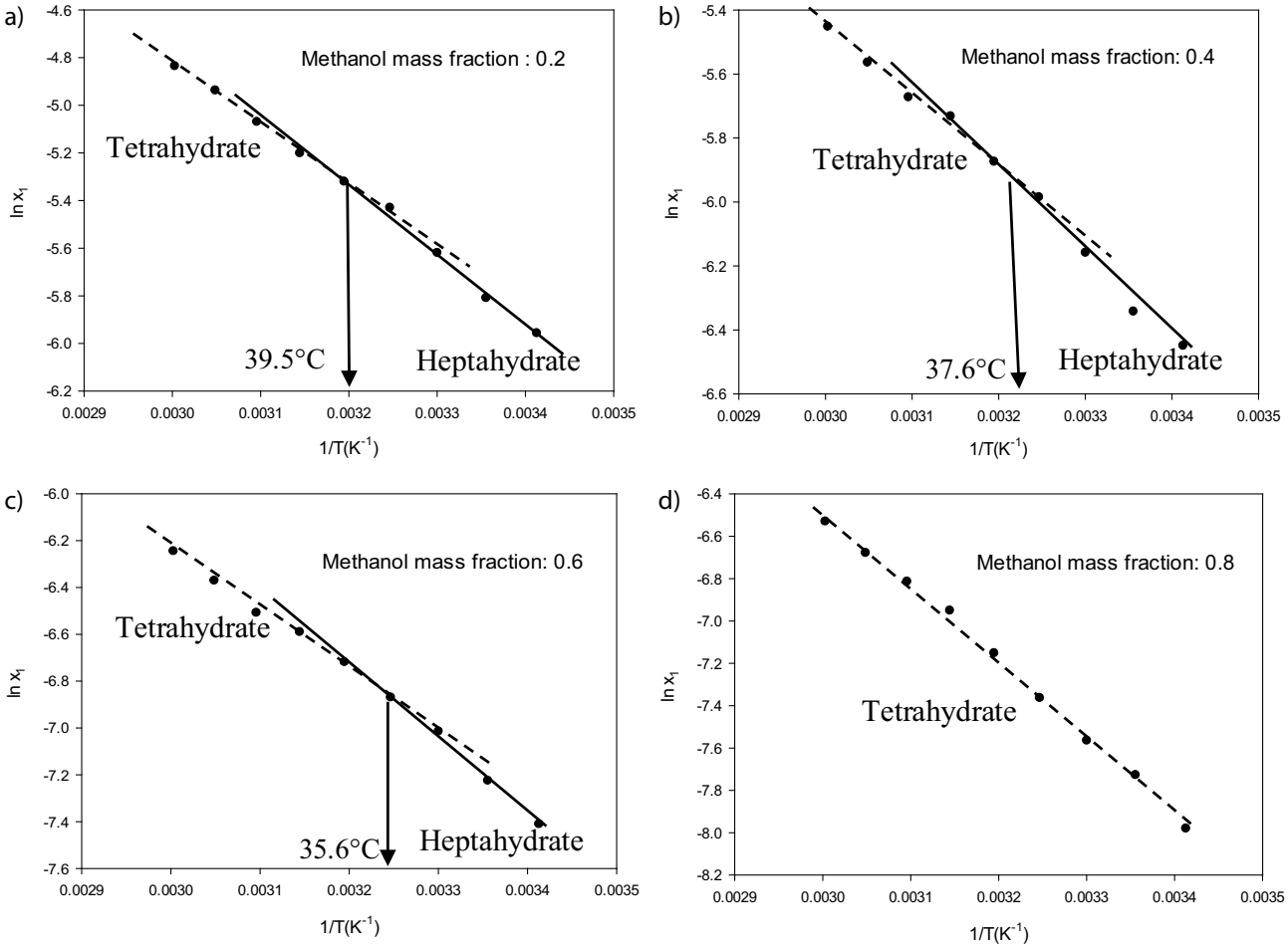

Figure 5. Plot of lnx_1 versus 1/T from the solubility of GMP at methanol fractions of (a) 0.2, (b) 0.4, (c) 0.6, and (d) 0.8. The R^2 of linear regression analyses is 0.994.

1) List of symbols at the end of the paper.

Table 2. Enthalpy and entropy of dissolution of the heptahydrate and tetrahydrate.

Methanol fraction [–]	Heptahydrate		Tetrahydrate		Transition temperature [°C]
	ΔH_d [kJ mol^{-1}]	ΔS_d [kJ mol^{-1}K^{-1}]	ΔH_d [kJ mol^{-1}]	ΔS_d [kJ mol^{-1}K^{-1}]	
0.2	21.7	0.0526	20.7	0.0491	39.5
0.3	22.0	0.0503	20.8	0.0464	39.1
0.4	22.1	0.0500	20.8	0.0448	37.6
0.5	21.0	0.0411	20.2	0.0386	37.4
0.6	24.6	0.0508	22.2	0.0429	35.6
0.7	29.8	0.0660	24.7	0.0499	30.1
0.8	–	–	27.9	0.0574	–
0.9	–	–	30.4	0.0612	–

exists without a transition point at a methanol mass fraction > 0.8.

3.2 Effect of the Solvent Fraction on the Maximum Supersaturation

Examples of maximum supersaturated concentrations measured by Raman spectroscopy and FBRM in anti-solvent crystallization are shown in Fig. 6, which presents the concentrations of the solution and the concentrations of the solid forms. The transformation of the amorphous form to the heptahydrate can be clearly observed from the Raman shift, as shown in Fig. 6a. The operation was performed by adding methanol (methanol/water ratio of 1:1) for 10 s to a solution at a GMP/solvent ratio of 0.2 and 20 °C. The formation of amorphous GMP was observed first, as soon as the methanol was added. After 4607 s, transformation into a heptahydrate crystal started, and the transformation was finished at 8354 s. The supersaturated concentrations of the amorphous and heptahydrate solids were 0.1263 and 0.0503, respectively. An instant addition resulted in maximum supersaturation in anti-solvent crystallization. In these experiments, the number of particles increased rapidly during nucleation and the particle size was 5–10 µm, but the number of particles decreased and the particle size increased when the heptahydrate was formed.

The transformation of the heptahydrate into the tetrahydrate was clearly observed from the Raman spectra results, as depicted in Fig. 6b. The operation was performed by adding methanol (methanol/water ratio of 1:1) for 10 s in the solution concentration (GMP/solvent of 0.2) at 50 °C. Heptahydrate GMP was first formed after 3 s and then transformation into tetrahydrate crystals started after 5290 s and was completed at 7231 s. The supersaturated concentrations of the heptahydrate and tetrahydrate crystals were 0.0646 and 0.0532, respectively. The average of the points where the concentration was stable before the phase transition started was considered as the metastable form solubility. The metastable region (concentration) was measured at a constant temperature and mass fraction of methanol. The metastable region had the largest supersaturation for the amorphous form and there was only little difference between tetrahydrate and heptahydrate. It was observed that, when the mass fraction of methanol is greater than 0.8, the supersaturated concentrations of the tetrahydrate and heptahydrate are almost the same.

In another example, the operation was performed at 50 °C with a methanol mass fraction of 0.7 and a GMP/solvent ratio of 0.2 by adding methanol instantly (Fig. 6c), and the results show that amorphous GMP was generated instantly after methanol addition. Transformation into a heptahydrate crystal started after 280 s, followed by transformation into the tetrahydrate after 698 s. The maximum supersaturation of the amorphous, heptahydrate, and tetrahydrate solids was measured as the difference between the actual concentration and the equilibrium concentration (saturation). This supersaturated concentration represents a characteristic value for each form and is: amorphous ≫ heptahydrate > tetrahydrate. The stability is: tetrahydrate > heptahydrate ≫ amorphous, and the solubility tends to be reversed so that it can be assumed that the supersaturation of the solid forms is generated.

The amorphous solid form was expected to be detected during rapid addition, and the heptahydrate or tetrahydrate crystals, by slow addition. Under intermediate conditions, polymorphic transformation was confirmed. The mixing of all polymorphic forms was not detected in any experiment, except for transformation. It is recognized that the Raman method is very likely to detect less than 1 % of solid state impurities. There was some delay between the nucleation point and the reaction of the Raman probe at a slow input rate, but the trend was clearly analyzed. This was due to the time required for sufficient solids to accumulate in the solution. The off-line X-ray diffraction results of the solids recovered at the end of the crystallization were consistent with the Raman results for the different solid forms. The concentration at that time was also consistent with the Raman results.

The solubilities and maximum supersaturation concentrations of the three solids, which were measured by anti-solvent crystallization, are shown in Fig. 7, with the solubility and maximum supersaturation against the methanol mass fraction at 20 and 50 °C being shown in Figs. 7a and 7b, respectively. The amorphous solubility was highest over the entire solvent fraction range. On the other hand, the solubilities of the tetrahydrate and heptahydrate were similar, with that of the tetrahydrate being slightly lower. The maximum supersaturation was highest in the amorphous form, followed by the heptahydrate and tetrahydrate. From these results, the solubility and maximum supersaturation values to selectively produce the amorphous, heptahydrate, and tetrahydrate forms were clearly provided. The amorphous solid form was generated at the highest supersaturation compared to the hydrates. Heptahydrate crystallization was possible at 20–40 °C and a methanol fraction of 0.15–0.6. The tetrahydrate was obtained in the

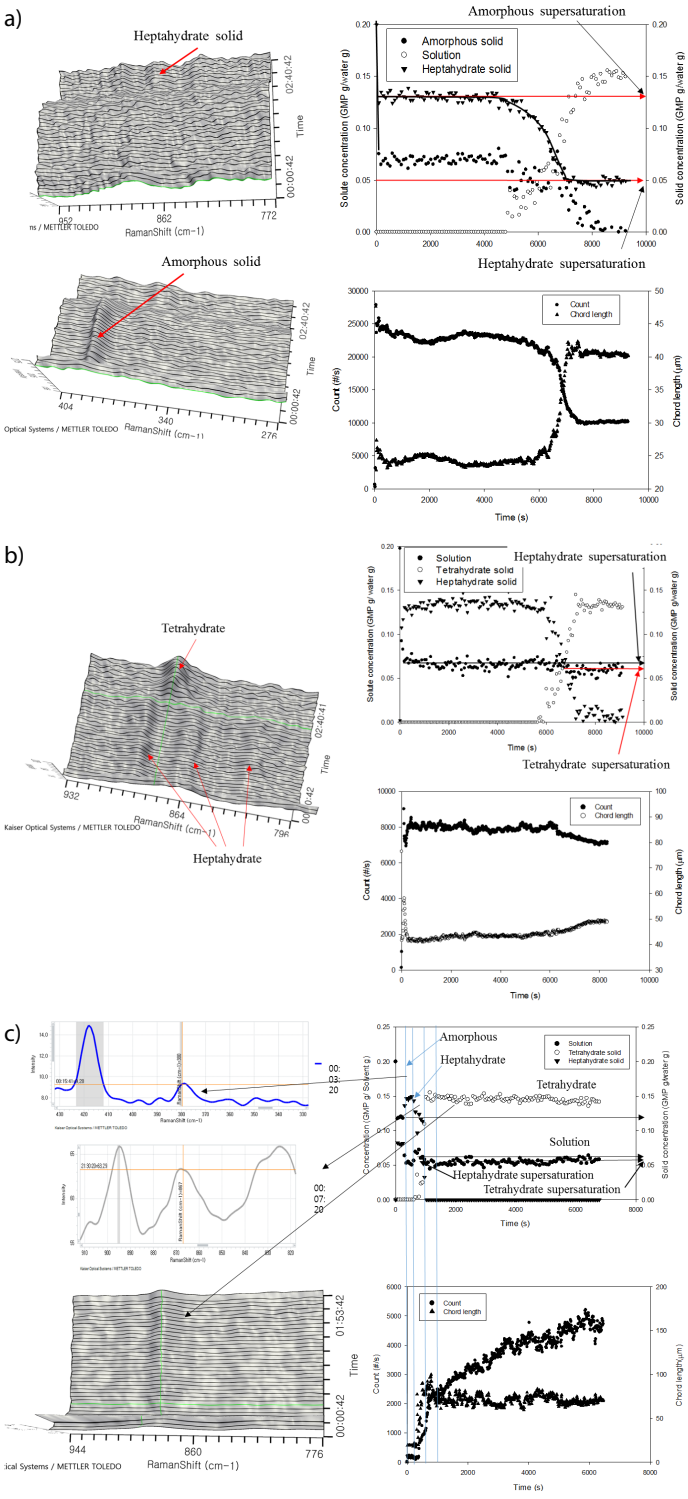

Figure 6. Measurement of the maximum supersaturated concentrations of (a) the amorphous and heptahydrate forms using anti-solvent crystallization by Raman spectroscopy and FBRM at 20 °C and a methanol fraction of 0.5; (b) the tetrahydrate and heptahydrate using anti-solvent crystallization by Raman spectroscopy and FBRM at 50 °C and a methanol fraction of 0.5; (c) the amorphous form, tetrahydrate, and heptahydrate using anti-solvent crystallization by Raman spectroscopy and FBRM at 50 °C and a methanol fraction of 0.7.

entire solvent fraction range at 45–60 °C and, especially, was crystallized when the methanol fraction was 0.8 or higher, even in the range of 20–40 °C.

Solubility is a thermodynamic property, but the maximum supersaturation or upper limit of the metastable zone is a kinetic property. The actual supersaturation depends on the rate of crystallization, since the metastable limit, i.e. the difference between solubility and actual supersaturation, depends on crystallization conditions. Information on the metastable limit is essential for the selective formation of hydrates and amorphous forms. In this study, it is revealed that crystalline selectivity can be identified by in-situ measuring the metastable limit. The kinetic studies are necessary for control of the crystal size, purity, shape, etc. Crystallization starts when the solution reaches supersaturation, and the crystal size, purity, shape, etc. are controlled according to the degree of this supersaturation. Therefore, supersaturation can be calculated using the solubility data established in this study, and crystalline and amorphous forms can be selectively produced by anti-solvent crystallization operation. Therefore, supersaturation can be predicted using the solubility data established in this study, and crystalline and amorphous forms can be selectively produced by anti-solvent crystallization operation. This will be continued to be reported in a subsequent study.

4 Conclusions

The solubilities and maximum supersaturated concentrations for the amorphous, tetrahydrate, and heptahydrate forms of GMP were determined by in-situ measurement using Raman spectroscopy and FBRM. The effects of the temperature and the solvent fraction were investigated. Calibrations between the concentrations and the Raman intensity were used to measure the solubility of GMP in binary solvent mixtures. The concentrations of the solid forms were correlated with calibration by Raman spectroscopy and monitored in situ by Raman spectroscopy. The thermodynamic properties and formation conditions for the amorphous, heptahydrate, and tetrahydrate forms were revealed. Combined with the PXRD, Raman, SEM, and TGA-DSC results, it was concluded that amorphous GMP, tetrahydrate GMP, and heptahydrate GMP can all be well characterized. The solubility and supersaturation limit for the tetrahydrate form crystallization were clarified. The dependence of the relative stabilities of the amorphous, tetrahydrate, and heptahydrate solids on the solvent composition and temperature as well as thermodynamic properties such as the enthalpy and entropy of dissolution of GMP were estimated by plotting the solubility data and temperature using the van't Hoff equation. Finally, the supersaturated concentrations and solubilities of hydrated GMP for different temperatures and solvent fractions were successfully determined by in-situ Raman spectroscopy and FBRM. It was shown that the use of these in-line tools can provide solubility and maximum supersaturation values to selectively produce amorphous, heptahydrate, and tetrahydrate solids. Heptahydrate crystallization is possible at

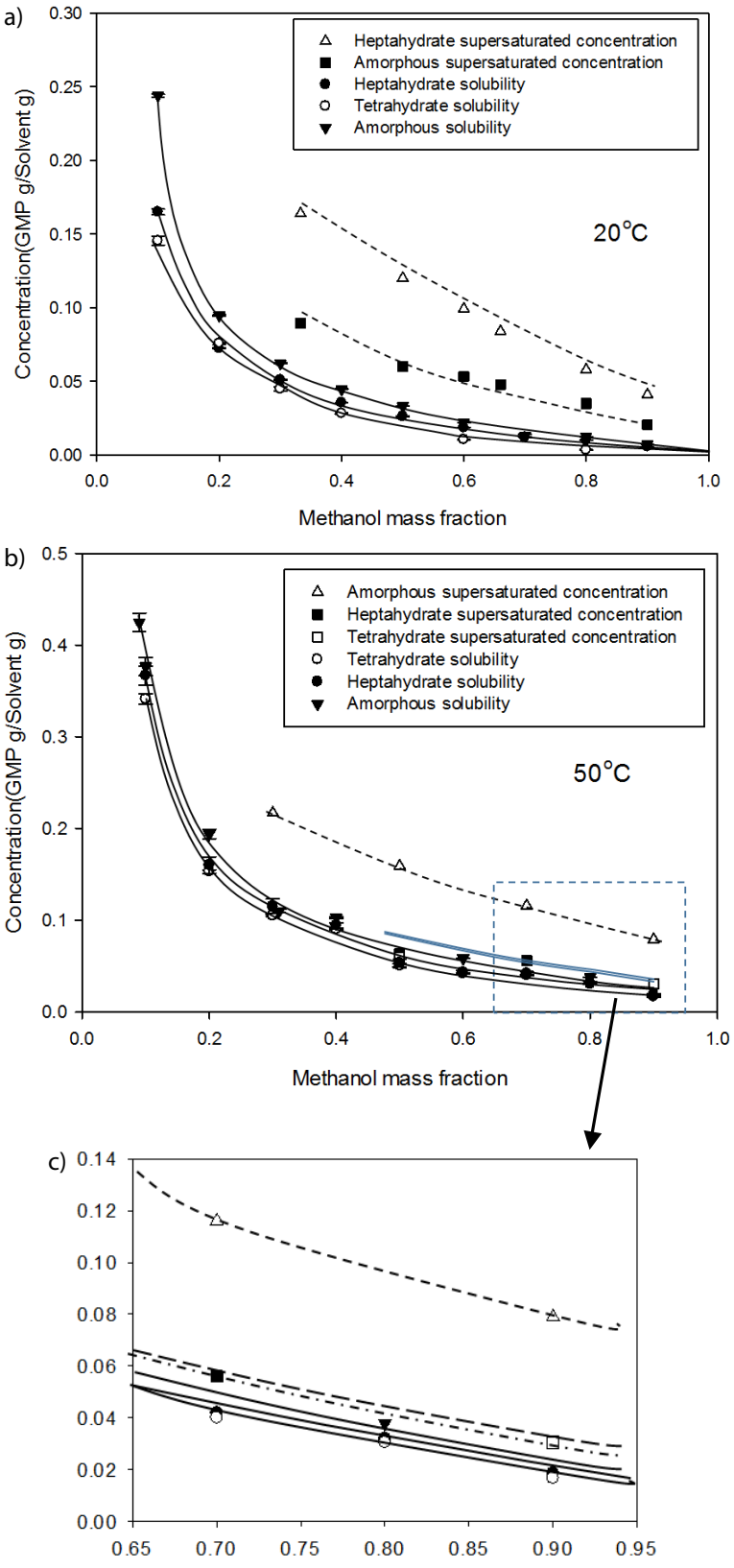

Figure 7. Solubility and maximum supersaturated concentration of the amorphous, heptahydrate, and tetrahydrate forms at (a) 20 and (b, c) 50 °C.

20–40 °C and a methanol fraction of 0.15–0.6. The tetrahydrate can be obtained in the entire solvent fraction at 45–60 °C and, especially, is crystallized when the methanol fraction is 0.8 or higher, even in the range of 20–40 °C. As a result, it is possible to provide the fundamental data for crystallization of the hydrates, enabling to obtain the desired hydrate by measuring the solubility and supersaturation of the crystalline and amorphous forms using in situ Raman and FBRM analysis.

Supporting Information

Supporting Information for this article can be found under DOI: https://doi.org/10.1002/ceat.202100260.

The authors have declared no conflict of interest.

Symbols used

ΔH_d	[kJ mol^{-1}]	dissolution enthalpy
R	[kJ mol^{-1}K^{-1}]	gas constant
ΔS_d	[kJ mol^{-1}K^{-1}]	dissolution entropy
T	[K]	absolute temperature
X	[–]	mole fraction

Abbreviations

DSC	differential scanning calorimetry
FBRM	focused beam reflectance measurement
PXRD	powder X-ray diffraction
SEM	scanning electron microscopy
TGA	thermogravimetric analysis

References

[1] J. Ulrich, *Chem. Eng. Technol.* **2003**, *26*, 832–835.
[2] B. Bechtloff, S. Nordhoff, J. Ulrich, *Cryst. Res. Technol.* **2001**, *36*, 1315–1328.
[3] J. Ulrich, M. Pietzsch, *Cryst. Res. Technol.* **2015**, *50*, 560–565.
[4] S. B. Zimmerman, *J. Mol. Biol.* **1976**, *106 (3)*, 663–672.
[5] S. Katti, T. Seshadri, M. Viswamitra, *Curr. Sci.* **1980**, *49 (14)*, 533–535.
[6] Q. Chen, F. Zou, P. Yang, J. Zhou, J. Wu, W. Zhuang, H. Ying, *Chin. J. Chem. Eng.* **2018**, *26*, 2112–2120.
[7] F. Zou, Q. Chen, P. Yang, J. Zhou, J. Wu, W. Zhuang, H. Ying, *Ind. Eng. Chem. Res.* **2017**, *56*, 8274–8282.
[8] B. S. Liu, H. Sun, J. K. Wang, Q. X. Yin, *Food Chem.* **2011**, *128*, 218–221.
[9] R. Zhang, J. Ma, J. Li, Y. Jiang, M. Zheng, *Fluid Phase Equilib.* **2011**, *303*, 35–39.

[10] B. S. Liu, H. Sun, J. K. Wang, Q. X. Yin, *Fluid Phase Equilib.* **2014**, *370*, 58–64.
[11] H. O. Yang, J. H. Kim, K. J. Kim, *Propellants, Explos., Pyrotech.* **2020**, *45*, 422–430.
[12] D. L. T. Nguyen, K. J. Kim, *Chem. Eng. Technol.* **2015**, *38*, 1059–1067.
[13] J. Ulrich, M. J. Jones, *Chem. Eng. Res. Des.* **2004**, *82 (A12)*, 1567–1570.
[14] Z. Fang, L. Zhang, S. Maob, S. Rohani, J. Ulrich, J. Lu, *J. Chem. Thermodyn.* **2015**, *90*, 71–78.
[15] I. H. Park, H. O. Yang, J. H. Kim, K. J. Kim, *Cryst. Growth Des.* **2019**, *19*, 4990–5004.
[16] M. A. O'Mahony, D. M. Croker, Å. C. Rasmuson, S. Veesler, B. K. Hodnett, *Org. Process Res. Dev.* **2013**, *17*, 512–518.
[17] J. Guo, M. J. Jones, J. Ulrich, *Chem. Eng. Res. Des.* **2010**, *88*, 1648–1652.
[18] H. Kamio, H. Nakamachi, *Yakugaku Zasshi* **1967**, *87*, 1436.
[19] C. L. Barnes, S. W. Hawkinson, *Acta Cryst.* **1982**, *B38*, 812–817.
[20] M. Tsubonoya, A. Murofushi, S. Yamamura, Y. Sugawara, *Struct. Chem.* **2018**, *74*, 1153–1159.
[21] H. Qu, M. Louhi-Kultanen, J. Kallas, *Int. J. Pharm.* **2006**, *321*, 101–107.
[22] T. N. P. Nguyen, K. J. Kim, *Int. J. Pharm.* **2008**, *364*, 1–8.
[23] W. Su, H. Hao, M. Barrett, B. Glennon, *Org. Process Res. Dev.* **2010**, *14*, 1432–1437.
[24] N. Wang, Q. Fu, G. Yang, *Fluid Phase Equilib.* **2011**, *306*, 171–174.
[25] D. Murphy, F. Rodríguez-Cintrón, B. Langevin, R. C. Kelly, *Int. J. Pharm.* **2002**, *246*, 121–134.

